Thermal Simulation of Nanosecond Laser Annealing of 3D Sequential VLSI

Benoît Mathieu, Claire Fenouillet-Beranger, Sébastien Kerdiles, Jean-Charles Barbé
Univ. Grenoble Alpes
CEA, LETI, MINATEC Campus
Grenoble, France
benoit.mathieu@cea.fr

***Abstract*—A framework for the simulation of nanosecond laser annealing of structures found in 3D sequential integration is presented. The framework includes a finite difference frequency domain Maxwell solver and a Poisson solver for the thermal diffusion. Simple applications illustrate the advantages, expected difficulties and optimization levers of this annealing technique.**

Keywords—nanosecond laser; annealing; melt; simulation; 3D sequential integration; CoolCube^{TM}

I. Introduction

Due to its low in-depth thermal diffusion, nanosecond laser annealing is a promising opportunity to achieve top transistor dopant activation in 3D sequential integration, as it provides both high dopants activation together with surface confined heating. With an interlayer spacing in the 100 nm range, laser pulses shorter than 100 to 200 ns will provide a selective heating of the top layer and preserve the already built bottom layer of transistors and inter-level interconnections. However, large temperature differences between layers are obtained at the expense of temperature uniformity inside the top layer. The modeling of the local thermal budget seen by different parts of the structure becomes mandatory to understand and optimize the laser annealing process. Contrary to bulk silicon, where heat diffuses on much longer distances than the absorption length of the light, thin films and stacked structures insulated with silicon oxide are subject to localized heating where the laser energy is absorbed depending on the laser wavelength and optical properties of the structure materials. This is due not only to the different light absorption length but also to the complex interferences between the incident wave and the ones reflected by the lower interfaces. Hence, computing a 2D or 3D electromagnetic model of the wave propagation in the 3D structure is mandatory. Another difficulty for modelling is the dependence of optical and thermal properties of the materials on the temperature. A simulation framework has been built and some results have been recently presented in [1] where its accuracy versus experimental results has already been highlighted. In this paper, we describe in more details the numerical simulation method and we apply it to various structures in order to optimize the materials and geometry for laser annealing in 3D sequential integration.

II. Numerical method

A simulation framework of nanosecond pulsed laser annealing has been developed at LETI. The laser wave propagation and absorption is computed with a finite difference frequency-domain Maxwell solver written in C++. Despite of its high computational cost, it takes just a few minutes to compute the steady state wave propagation in a 2D domain of 500x4000 cells of 1 nm. This mesh size is appropriate to model one or two transistors with either green or UV lasers available in the industry. The input of the Maxwell solver is, for each mesh cell, a material index and the temperature. The solver also needs the wavelength and tables providing the temperature dependent complex refractive index for each material at this wavelength. With an optimized solver on a small parallel computer, 3D computations are accessible. The absorbed energy field is provided to an implicit finite element transient Poisson solver to compute the temperature field. The Poisson solver is based on the open source FreeFEM++ solver by F. Hecht [2]. The automatic mesh refinement feature of FreeFEM++ is used to produce meshes with 10,000 to 30,000 elements for the 2D structures being studied here. On such meshes, the Poisson solver computes several implicit time steps per minute for the typical simulation of 40 time steps shown on figure 1. The input of the Poisson solver is a database of temperature dependent material properties, a field of material indices, the pulse shape and the field of power density provided by the Maxwell solver. To take into account the change in optical properties with temperature, the Maxwell solver must be periodically run to update the power source term of the Poisson solver. The principles of such simulations have been presented in [3].

Some materials have a negative permittivity. This is the case for metallic materials, e.g. when the extinction coefficient k is larger than the real part n of the refractive index. These materials are for example copper, aluminum, melted silicon and amorphous silicon (at a wavelength of 308 nm). Finite difference time domain explicit methods, which are the simplest available, are unstable in this case. Therefore, we use the so-called finite difference frequency domain method with the time harmonic inverse iteration method described in [4].

978-1-4673-7860-4/15/$31.00 ©2015 IEEE

III. OPTICAL AND THERMAL PROPERTIES OF MATERIALS

A. *Optical properties*

In this work, we will mainly use data derived from [5]. There is a large uncertainty on the optical properties of materials at high temperature (especially above 900K), and doping can greatly modify these properties. We also don't take into account optical non-linearity that might arise at very high laser intensity. For all these reasons, the simulations presented here cannot be considered predictive at this stage but provide useful trends to understand and optimize the process. Optical properties used in this work are shown in table I.

We focus on two wavelengths: 532 nm which corresponds to a frequency doubled Nd:YAG laser, and 308nm which is the output of XeCl excimer laser. 532 nm corresponds to a photon energy lower than the direct band gap of crystal silicon (C-Si, 3.4 eV or 365 nm at room temperature). In this case, the optical absorption coefficient is low compared to that of the amorphous and liquid phases of silicon, and strongly increases with the temperature. Green lasers will selectively heat the amorphous phase of silicon while the crystalline phase will absorb less energy. 308 nm is representative of a regime where the optical absorption of all phases of the silicon is large and weakly dependent on the temperature. For wavelengths below 365 nm, all silicon phases have small and similar absorption lengths, which might be useful to selectively anneal the top layer of silicon on insulator (SOI) structures with silicon films thinner than 10 nm. The 532 nm wavelength is particularly challenging for the simulation: the amount of absorbed energy changes with the temperature and the absorption length strongly depends on the material composition (doping, possible germanium content), temperature and phase. An accurate modelling of the phase transitions is therefore needed, as well as comprehensive database of refractive indices. This work uses a partial dataset but interesting conclusions can be drawn from the simulation results.

B. *Thermal properties*

The thermal properties used in this work are summarized in table II. The conductivity of the crystal silicon strongly decreases with the temperature. It is also known that the thermal conductivity of thin silicon films is anisotropic and much lower than the thermal conductivity of bulk materials due to confinement effects. At this scale a thermal contact resistance must also be taken into account at interfaces between different materials. The two latter effects are not modeled in this work and the data will have to be completed and calibrated using experimental results.

TABLE I. OPTICAL PROPERTIES USED IN THIS WORK

Material	λ=308 nm			λ=532 nm		
	n	***k***	***1/α*[nm]**[a]	***n***	***k***	***1/α*[nm]**
C-Si 300K	5.07	3.62	6.8	4.11[b]	0.043[c]	995
C-Si 900K				4.37	0.16	260
C-Si 1600K				4.7	0.9	47
Amorph-Si	2.7	3.4	7.2	4.7	1.3	32
Liquid-Si	1.27	3.75	6.5	2.35	4.8	8.8
Silicon oxyde	2.2	0	∞	1.57	0	∞
Silicon nitride	2.15	0	∞	2	0	∞
Copper	1.39	1.67	15	0.8	2.5	17

[a] Absorption length, with $\alpha = 4\pi k/\lambda$
[b] The optical refractive index is a linear function of temperature
[c] The absorption coefficient k is an exponential function of temperature

TABLE II. THERMAL PROPERTIES USED IN THIS WORK

Material	*Mass density (kg/m^3)*	*Thermal conductivity (W/m/K)*	*Heat capacity (J/kg/K)*
C-Si	2350	156 @300K 43 @800K 24 @1400K	700 @300K 870 @800K 970 @1400K
Amorph-Si	2330	2.4 @300K 3.7 @800K 4.5 @1400K	720 @300K 880 @800K 970 @1400K
Silicon oxyde	2650	1.5 @400K 1.7 @600K 2.2 @800K 2.9 @1000K	900
Silicon nitride	3200	10	900
Copper	8960	400	400

IV. OPTICAL EFFECTS IN THE 3D SEQUENTIAL STRUCTURES

Nanosecond laser annealing of thin film structures in general involves complex optical effects, especially when the light is partially transmitted through the first layer of silicon. Several phenomena must be taken into account to optimize the annealing process. A few examples are given below.

A. *Temperature dependent optical properties of the material*

This topic is particularly important for thin crystalline silicon films on insulator and wavelengths larger than 365 nm. Such a structure has a large absorption length at room temperature, at the beginning of the annealing sequence, which decreases as soon as the temperature reaches 1200K. Fig. 1 shows the profile of absorbed energy density on a typical SOI structure at different uniform temperatures. Above 1200K, the absorption length of the silicon decreases significantly. This behavior can be used to selectively anneal the upper layers of stacked structures, however amorphization provides an even better contrast to selectively heat the structures that have to be annealed.

Optical properties also strongly change due to phase change of the material. This will be illustrated in the next section.

B. *Reflection coefficient of the structure*

The reflection coefficient determines the total amount of energy absorbed by the structure. Fig. 2 demonstrates how the reflection coefficient changes with the thickness of a top silicon nitride coating and at different stages of the annealing. The amorphous silicon is sometimes considered melted above 1500 K (but optical properties are uncertain). We assume that this undercooled liquid recrystallizes very quickly, similarly to solid phase expitaxial regrowth. According to [6], the velocity of the amorphous/crystalline interface could exceed 1 m/s at 1500 K and a total recrystallization of a 20 nm film is possible with only one pulse of 40-100 ns. If the structure is further heated, the temperature can exceed the melting point of the crystal silicon and the optical properties change again. The reflection coefficient of the structure is a periodic function of the coating thickness. The curves indicate that the properties of the coating (material and thickness) can be adjusted to optimize the amount of energy absorbed at the different stages of the annealing process. To enlarge the process window, situations where the amount of absorbed energy increases at high temperature (for example a strong decrease of the reflectivity above the melting temperature) should probably be avoided. Of course, these results are strongly dependent on the optical properties of the materials, the temperature distribution and the thicknesses of the different layers.

C. *Optical effect of buried structures*

When part of the laser beam reaches the lower layers, reflection and interference occur in the buried oxide layers. In this case, the amount of energy absorbed by the different parts of the structure depends on the geometry and materials below, as illustrated on Fig. 3. Light is reflected by the different optical interfaces below the top silicon film. The incident and the reflected waves interfere and this results in a complex profile of deposited energy. This profile as well as the total amount of absorbed energy in the top layer are in some cases very sensitive to the optical properties, wavelength and geometry. Again, this proves that solving the Maxwell equations is necessary to understand the annealing process of 3D sequential integration structures.

D. *Two dimensional optical effects*

In the 3D sequential integration, complex patterned structures will be annealed, mainly in order to activate the dopants in the source and drains of the transistors. If the gate stack is already built, diffraction and absorption occur in the gate stack and create a non-uniform power density in the source and drains. The source and drain regions should however be heated at a uniform temperature while the gate stack, the bottom layers of transistors and the interconnections must be kept below a safe temperature limit.

Fig. 4 represents the field of absorbed power density for two structures and two different wavelengths. The choice of the wavelength has a strong impact in this case: due to its small absorption length a UV laser will generally be less sensitive to phase changes, and structures below the upper layer of transistors (in this example the energy absorbed by the bulk silicon is ten times lower than with a green laser). A drawback of UV light is that the gate-stack sees a higher

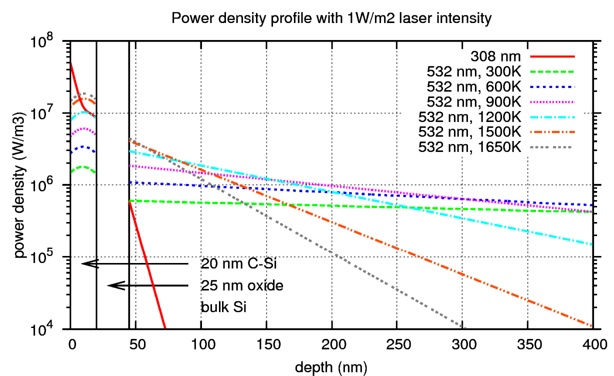

Fig. 1. Profile of absorbed laser energy in a silicon on insulator wafer (for a normalized laser intensity of 1 W/m2, the laser intensity of a 50 ns pulse of 1 J/cm^2 is 2x10^{11} W/m^2 and the power density must be scaled accordingly).

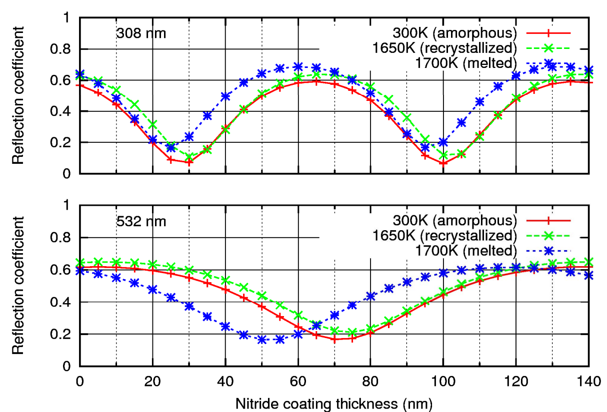

Fig. 2. Simulated reflection coefficient of a stack with a bulk silicon wafer, a 100 nm oxide layer, a 20 nm amorphized silicon film (with a thin crystalline seed layer), and a variable thickness nitride coating. When increasing the temperature, it is assumed that solid phase epitaxial regrowth (SPER) has recrystallized the film at 1650 K and that the film is melted at 1700 K.

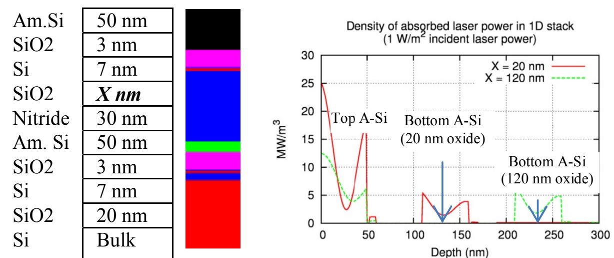

Fig. 3. Simple 1D structure illustrating complex reflections and interference effects in a multilayer. It is a vertical cut in the more complex structure studied in Fig. 4. The figure shows two cases: a thin buried oxide layer of X=20nm and a thicker one of X=120nm.

power density than the source and drain regions. On the contrary, the green laser light will be strongly absorbed by the pre-amorphized source and drain regions, and weakly absorbed by the poly-silicon gate stack. However a higher fraction of the energy also reaches the lower levels of transistors and interconnections. As a consequence, lower levels might reach higher temperatures, and the optimal laser

power is more sensitive to the geometry of buried structures because of the reflections on these structures.

Fig. 4 illustrates the effect of the presence of patterning and inter-level metallic connection lines on the power density field. A 30 nm nitride coating on the upper transistor reduces the reflection coefficient of the structure and increases the amount of energy absorbed by the source and drain regions in this case. An opening in the silicon film models a shallow trench isolation and allows some energy to reach the bottom levels. Interestingly, in this example, the maximum power density received by the metallic plane is located under the transistor and not under the opening. In this case, the shape of the upper transistor acts as a lens and concentrates the laser beam under the transistor. In this example, the addition of a copper plane below the top level transistor decreases the total energy absorbed by the top transistor by 25% with the 532 nm laser, while it is increased by 18% with the 308 nm laser.

However, the electromagnetic simulation alone is not sufficient to predict the thermal budget of the annealing step.

V. Thermal Effects

Fig. 5. shows the resulting temperature field at the end of a square laser pulse in the particular configurations shown on fig. 4. The thick silicon oxide layer provides an appropriate thermal insulation to preserve the bottom layer of transistors (the maximum temperature of the bottom transistor is 400°C in this case). In this example however, the copper plane absorbs a significant part of the laser energy and reaches 750°C with the 532 nm wavelength. Moreover, due to the non-uniformity of the power density in the upper transistor with this wavelength, the temperature is also non uniform (in the source/drain a temperature gradient between 1020 and 1200°C is observed). Also, a higher laser energy (0.21 J vs 0.164 J) is required in this case to reach 1200°C. The difference in laser energy to process different transistors, as well as the temperature gradients in the processed areas might affect dopants activation uniformity. Hence, in this example, the design should probably be changed for better results with the 532 nm laser while it seems appropriate for the 308 nm laser.

VI. Conclusion

This work demonstrates that a calibrated 2D or 3D numerical simulation is mandatory to understand and optimize the nanosecond laser annealing of structures found in the 3D sequential integration processes like CoolCube™. For instance, dopant activation in the source and drain regions of the transistors in a few tens of nanoseconds probably necessitates temperatures above 1200°C in these regions while the source, drain and gate stack must never be entirely melted. We demonstrated that the pulse energy required to reach a given temperature can be very sensitive to the geometry of the transistors. Hence, the coupled electromagnetic and thermal simulation of the laser annealing is an essential and complex step in the design. Accurate temperature dependent optical and thermal properties of the materials are required to produce predictive simulations.

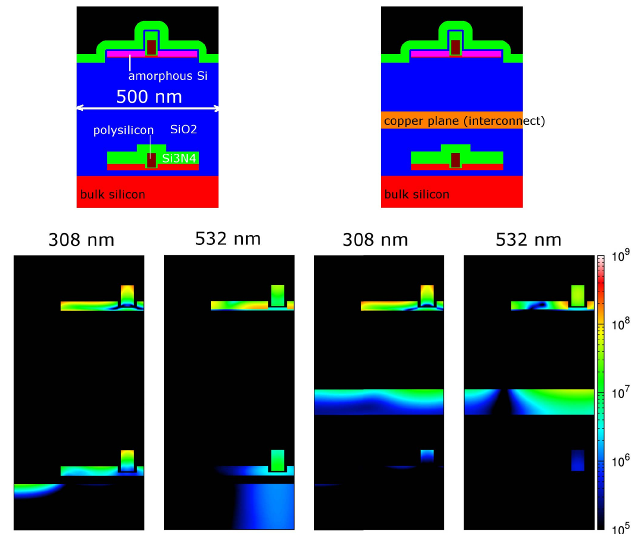

Fig. 4. Influence of the patterning and underlying interconnection layers on the power density field (in W/m3 for a 1 W/m2 incident wave). Two structures are shown, with and without a copper interconnection, and two laser wavelengths are shown for each structure.

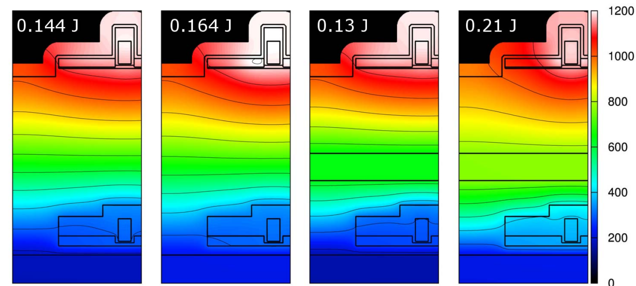

Fig. 5. Temperature field at the end of a 100 ns square pulse (conditions identical to Fig. 4). The indicated pulse energy has been adjusted to reach a maximum temperature of 1200°C in each case. Temperature in °C.

We have built a simulation tool with the required capabilities. The tool has been used to investigate the influence of laser wavelength, energy, material properties and geometry on the thermal budget. The optical and thermal properties will have to be completed and validated by comparison with experimental data, and the modelling of the phase change will have to be enhanced to represent the progressive recrystallization and melt of the silicon.

[1] C. Fenouillet-Beranger et al. "New insights on bottom layer thermal stability and laser annealing promises for high performance 3D Monolithic integration", IEDM 2014 (Conference paper)

[2] F. Hecht, "New development in FreeFem++," Journal of Numerical Mathematics, vol 20, 2012, pp. 251-265.

[3] G. Fisicaro, A. La Magna. "Modeling of laser annealing", *J Comput Electron*, vol. 13, pp. 70-94, March 2014.

[4] C. Pflaum and Z. Rahimi, "A finite difference frequency domain method (FDFD) for materials with negative permittivity," in Electromagnetics in Advanced Applications, ICEAA'09 (conference paper)

[5] R. F. Wood, C. W. White and R. T. Young, "Semiconductors and Semimetals, volume 23: pulsed laser processing of semiconductors," Academic Press, 1984 (book)

[6] R. Stiffler, P. V. Evans and A. L. Greer, "Interfacial transport kinetics during the solidification of silicon, " in Acta metall. Mater., vol. 40, no. 7, 1992, pp. 1617-1622